

# SCIENTIFIC REPORTS



OPEN

## Short and long time effects of low temperature Plasma Activated Media on 3D multicellular tumor spheroids

Florian Judée<sup>1,2</sup>, Céline Fongia<sup>3,4</sup>, Bernard Ducommun<sup>3,4,5</sup>, Mohammed Yousfi<sup>1,2</sup>, Valérie Lobjois<sup>3,4</sup> & Nofel Merbahi<sup>1,2</sup>

Received: 08 October 2015

Accepted: 22 January 2016

Published: 22 February 2016

This work investigates the regionalized antiproliferative effects of plasma-activated medium (PAM) on colon adenocarcinoma multicellular tumor spheroid (MCTS), a model that mimics 3D organization and regionalization of a microtumor region. PAM was generated by dielectric barrier plasma jet setup crossed by helium carrier gas. MCTS were transferred in PAM at various times after plasma exposure up to 48 hours and effect on MCTS growth and DNA damage were evaluated. We report the impact of plasma exposure duration and delay before transfer on MCTS growth and DNA damage. Local accumulation of DNA damage revealed by histone H2AX phosphorylation is observed on outermost layers and is dependent on plasma exposure. DNA damage is completely reverted by catalase addition indicating that H<sub>2</sub>O<sub>2</sub> plays major role in observed genotoxic effect while growth inhibitory effect is maintained suggesting that it is due to others reactive species. SOD and D-mannitol scavengers also reduced DNA damage by 30% indicating that O<sub>2</sub><sup>-•</sup> and OH<sup>•</sup> are involved in H<sub>2</sub>O<sub>2</sub> formation. Finally, PAM is able to retain its cytotoxic and genotoxic activity upon storage at +4 °C or -80 °C. These results suggest that plasma activated media may be a promising new antitumor strategy for colorectal cancer tumors.

Low temperature plasmas are weakly ionized gases involving various active species (reactive species, charged particles, long lived time excited species, UV radiation and also localized electric fields) diluted in neutral background gas at ambient temperature. Several different setups of low temperature plasma jets at atmospheric pressure can be found in the literature as for instance dielectric barrier discharges (DBD) monitored by pulsed or AC voltage<sup>1-3</sup>, corona discharges powered by DC or AC supply<sup>4,5</sup>, Radio-Frequency reactor<sup>6</sup> and Microwave plasmas<sup>7-9</sup>. Several carrier gases can be used to produce low temperature plasmas such as helium, argon, nitrogen, air or mixture of inert gases with air or N<sub>2</sub> or O<sub>2</sub>, or H<sub>2</sub>O, etc. Complex chemical kinetics is triggered by low temperature plasmas operating in open air at quasi-ambient temperature. The dominant radical species are likely to be formed from oxygen and nitrogen molecules leading to reactive oxygen species (ROS) and reactive nitrogen species (RNS), although other oxides due to the presence of humidity such as hydroxyl, hydrogen peroxide and hydroperoxyl radicals can also be produced.

Low temperature plasmas application to medicine has received increasing interest over the last decade<sup>10-17</sup>. In the case of neoplasia, low temperature plasmas operating in open air have been successfully tested, both *in vitro* and *in vivo*<sup>18-26</sup>. Recently, studies based on low temperature plasma conditioned culture media usually called Plasma Activated Medium (PAM) have demonstrated their activity on cancer cells. *In vitro*, PAM was shown to stop proliferation and induce DNA damage in HCT116 colon cancer cells<sup>20</sup>, to induce apoptosis on glioblastoma brain tumor cells<sup>27</sup>, to inhibit proliferation on human lung adenocarcinoma epithelial A549, human hepatocarcinoma HepG2 and mammary adenocarcinoma MCF-7 cells<sup>28</sup> and chronic chemo-resistant ovarian cancer cells<sup>29</sup>. *In vivo*, subcutaneous injection of PAM in murine tumor was reported to induce cytotoxicity against ovarian clear cell carcinoma<sup>30</sup> and suppress choroidal neovascularization in mice<sup>31</sup>. However, the active mechanisms and

<sup>1</sup>Université de Toulouse ; UPS, INP ; LAPLACE; 118 route de Narbonne, F-31062 Toulouse, France. <sup>2</sup>CNRS ; LAPLACE; F-31062 Toulouse, France. <sup>3</sup>Université de Toulouse; ITAV-USR3505, F-31106 Toulouse, France. <sup>4</sup>CNRS; ITAV-USR3505, F-31106 Toulouse, France. <sup>5</sup>CHU de Toulouse; F-31059 Toulouse, France. Correspondence and requests for materials should be addressed to N.M. (email: merbahi@laplace.univ-tlse.fr)

the identity of the chemical byproducts generated during conditioning of the culture media by the plasma and involved in these reported effects are either not well understood and nor clearly identified and quantified.

In the present study, we investigated the effects of liquid culture media conditioned during a short exposure time by pulsed He plasma jet on growth inhibition and the genotoxicity on HCT116 colorectal multicellular tumor spheroids (MCTS). The MCTS is a 3D culture model known as an intermediate stage in elaboration of anti-cancer therapy between classical *in vitro* (monolayer culture cells) and *in vivo* models<sup>20,32</sup>. We investigated more particularly the penetration effects of PAM not only on the outermost cells of MCTS but also inwards the inner regions. We also identified and quantified the specific role of H<sub>2</sub>O<sub>2</sub> and also the species involved by using several scavengers (catalase, SOD, D-mannitol and L-histidine) on DNA damage. Finally, we explored PAM stability and genotoxic and cytotoxic effects on MCTS upon storage at different temperatures and for duration varying from hours to several days.

## Results

**PAM retains genotoxic and cytotoxic effects in time transfer dependent manner.** We first considered a duration of exposure (Texp) of 120 s to generate PAM. HCT116 colon carcinoma multicellular tumor spheroids were transferred in PAM after increasing delay subsequent to the activation of culture media by the plasma jet (transfer times of 1 h, 14 h, 24 h and 48 h) and their growth was evaluated. Figure 1a displays the daily volume ratio between treated and untreated spheroids monitored during 9 days. Control spheroids, not exposed to PAM, grew as expected during the time of analysis (normalized ratio is 1). In contrast, growth of the spheroids cultivated in PAM was inhibited by about 40% in the case of short transfer times (1 h or 14 h). Growth inhibition appears to be dependent on the time transfer of the spheroid in PAM after preparation and indicates that two phases are involved in this inhibition. The first one occurs during the first day with a rapid decrease of MCTS volume followed by slower volume decrease the next days. For longer transfer times, spheroid volume decreases continuously and reaches about 20% of loss 9 days after spheroid transfer in PAM.

In order to assess DNA damage induced by PAM, spheroids were exposed after the same transfer times (1 h, 14 h, 24 h and 48 h) for 4 hours before fixation. Immuno-detection of phosphorylated form of histone H2AX was performed<sup>20</sup>. As shown in Fig. 1b, phosphorylated histone H2AX was detected in spheroids grown in PAM indicating that PAM induces DNA damage. Intense staining was detected in outermost region of spheroid treated by PAM in the case of time Ttrans = 14 hours. This staining was gradually decreases in the case of Ttrans = 24 h and was not detectable in spheroid grown in PAM for Ttrans = 48 h.

Together, these results indicate that PAM displays a genotoxic activity and inhibits growth. Furthermore, genotoxic activity appears to decrease along time and is barely detectable after 48 hours storage of PAM at 37 °C.

**DNA damage is dependent on the exposure time of culture media to plasma jet.** Exposure time (Texp) of the culture media to the He plasma jet is likely to be a key parameter in PAM activity on growth inhibition and DNA damage. To investigate this issue, culture media was exposed from 60 s to 240 s to He plasma jet. Spheroids were then grown in PAM and the DNA damage inducing effect was evaluated. Figure 2 displays representative cryosections of spheroids grown for 4 h in 3 types of PAM (Texp = 60 s, 120 s and 240 s) prepared 24 h and 48 h before the exposure of the spheroids. In the case of time Ttrans = 24 h, DNA damage detected in the outmost region of HCT116 spheroids increase in a plasma jet exposure time (Texp) dependent manner. For Texp = 60 s, only few sparse fluorescent spots were observed indicating limited DNA damage while in contrast the staining is strongly intense in spheroid treated by PAM activated during 240 s. In the case of a transfer after 48 h DNA damage is observed only in the case of 240 s exposure time. Thus, these data indicate that plasma jet exposure produces chemically reactive species in the culture medium in a time exposure-dependent manner.

**H<sub>2</sub>O<sub>2</sub> plays a major role in DNA damage of multi cellular tumor spheroids.** Low temperature plasma jet induces complex kinetic reactions between gaseous plasma species and the culture medium leading to the generation of many aqueous chemically reactive species with long lifetime. We have chosen to emphasize the role of more particularly H<sub>2</sub>O<sub>2</sub>, which is one of these chemical species already highlighted in the literature<sup>33</sup>.

To this aim we first examined whether the putative effect of oxidative hydrogen peroxide molecules in PAM culture media could be neutralized by catalase addition, an enzyme known to catalyze decomposition of hydrogen peroxide into water and oxygen<sup>34</sup>. We first examined DNA damage of spheroid induced by PAM in the presence of catalase (30 μg.mL<sup>-1</sup>). Catalase was also added in culture media of control spheroid to observe a possible direct effect of catalase on spheroids. As shown in Fig. 3b, DNA damaging effect of PAM is fully reversed by the presence of catalase. In all transfer time conditions (1 h to 48 h), no growth staining of phosphorylated-histone H2AX was detected on spheroids. However, unexpectedly, a moderate growth inhibitory effect was still observed (Fig. 3a) even if the absence of DNA damage. Altogether, these data confirm that H<sub>2</sub>O<sub>2</sub> is the major species involved in DNA damage observed in HCT 116 MCTS treated with PAM.

The generation pathway of H<sub>2</sub>O<sub>2</sub> in PAM can be attributed to the reaction of short-lived ROS produced in liquid medium when impacted by the gaseous plasma species. The most important ROS that can be generated in the present case are hydroxyl radical, superoxide anion radical, and singlet molecular oxygen. In order to estimate the production rates of these species (OH•, O<sub>2</sub><sup>-•</sup> and O<sub>2</sub>(<sup>1</sup>Δg)) involved in H<sub>2</sub>O<sub>2</sub> formation, different scavengers were added into culture media just before plasma exposure. Superoxide dismutase (SOD) is an enzyme that allows quenching of superoxide (O<sub>2</sub><sup>-•</sup>) to following a redox cycle by using a metallo-organic complex of copper, manganese, iron or nickel<sup>35</sup>. The hydroxyl radical (OH•) can react with itself in aqueous phase to produce hydrogen peroxide following a free-radical recombination. To quench this reaction, D-mannitol<sup>36</sup> is added before plasma treatment in culture medium. For a similar objective, L-histidine is added to the medium before treatment to quench singlet molecular oxygen<sup>37</sup> (O<sub>2</sub>(<sup>1</sup>Δg)). The concentrations of the added scavengers in media before plasma jet treatment are summarized in Table 1.

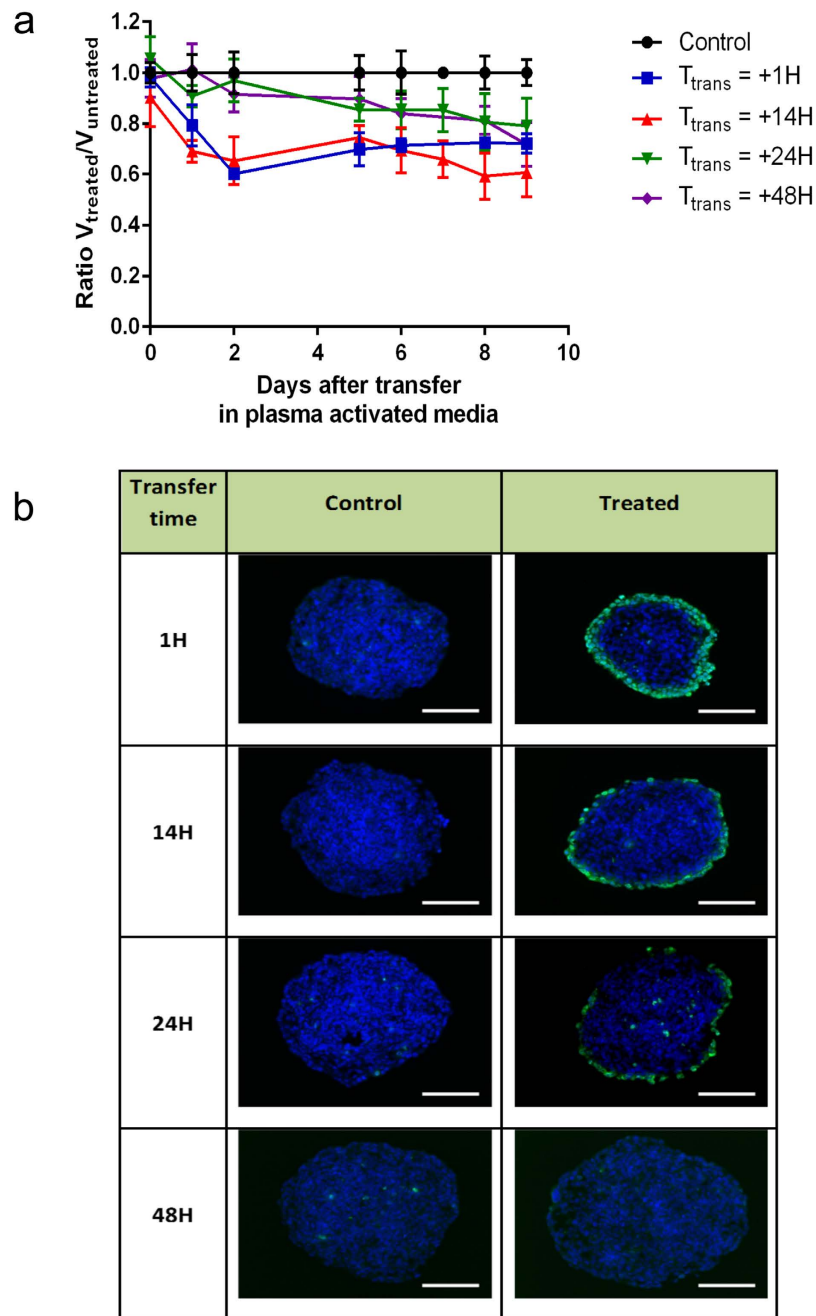


**Figure 1. Growth inhibition and genotoxic effects of PAM on HCT116 MCTS.** (a) Relative growth of spheroid after PAM treatment ( $T_{exp} = 120$  s) for several transfer times  $T_{trans}$ . The spheroids were cultured during five days in DMEM and transferred in PAM at day 0. Data are shown as means  $\pm$  SD from four independent experiments. (b) Genotoxic effect of PAM detected 4 h after transfer time of MCTS in PAM. Immuno-detection of the phosphorylation of the histone variant H2AX (phospho-H2AX, green) on  $5\ \mu\text{m}$  cryosections of control spheroids or treated spheroids. DAPI (blue) correspond to the Nuclei. Data shown are representative images from four independent experiments. Scale bar,  $100\ \mu\text{m}$ .

In these experimental conditions we examined DNA damage after exposure to PAM. As presented in Fig. 4, DNA damage was still detected in PAM exposed spheroids, however the effect of PAM appeared limited to the outermost layer of cells in presence of SOD, D-mannitol, while the effect of L-Histidine was not obvious.

A detailed analysis of these images with the Image J software allows quantifying the percentage of spheroid volume in which DNA damage is detected upon exposure to PAM. The DNA damage volume was  $33.6 \pm 3.5\%$  for spheroid grown in PAM,  $22.8 \pm 1.12\%$  in PAM with SOD (scavenger of  $\text{O}_2^{\bullet-}$ ),  $23.5 \pm 2.4\%$  with D-mannitol (scavenger of  $\text{OH}^{\bullet}$ ) and finally to  $29.5 \pm 1.6\%$  with L-histidine (scavenger of  $\text{O}_2(1\Delta\text{g})$ ). The DNA damaged spheroid volume is clearly dependent on scavenger type. Indeed, trapping of superoxide anion or hydroxyl radical reduces DNA damage of about 30% compared to the case of MCTS grown in PAM without scavenger. In the case of SOD

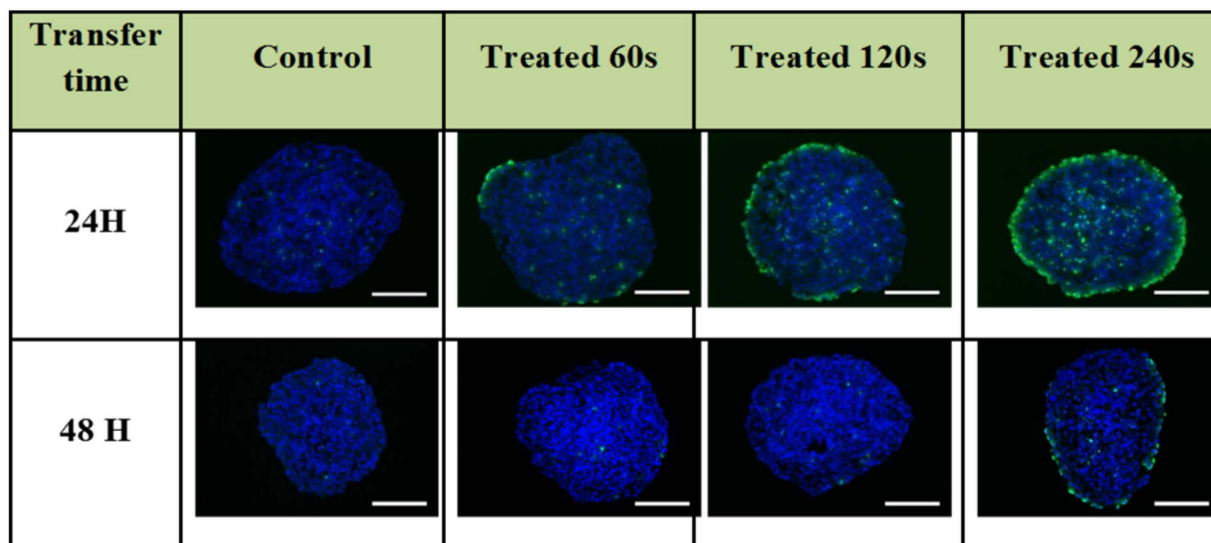


**Figure 2. Genotoxic effect of PAM prepared following increasing exposure duration ( $T_{exp} = 60$  s, 120 s and 240 s).** MCTS were transferred in plasma-activated medium after 24 h or 48 h, and fixed 4 h later. Immunodetection of the phosphorylated form of histone H2AX (phospho-H2AX, green) on  $5\ \mu\text{m}$  cryosections of control or treated spheroids. DAPI (blue) correspond to the Nuclei. Data shown are representative images from four independent experiments. Scale bar,  $100\ \mu\text{m}$ .

this proportion is more important because SOD-catalyzed dismutase superoxide to product either molecular oxygen ( $\text{O}_2$ ) or hydrogen peroxide ( $\text{H}_2\text{O}_2$ ). These results indicate that  $\text{O}_2^{\bullet-}$  and  $\text{OH}^{\bullet}$  are involved in the production of hydrogen peroxide in PAM. In contrast, given the limited reduction of DNA damage observed with L-Histidine scavenger, the singlet oxygen does not seem to play a significant role in the production hydrogen peroxide.

**Evaluation of  $\text{H}_2\text{O}_2$  concentration produced in PAM by He plasma jet.** In order to confirm the involvement of  $\text{H}_2\text{O}_2$  in the induction of DNA damage on MCTS cultured in the presence of PAM, we evaluated the effect of  $\text{H}_2\text{O}_2$  addition (initial solution from 30 wt. % in  $\text{H}_2\text{O}$ , Sigma) to culture medium without any prior plasma treatment. Both DNA damage and growth inhibition on the MCTS were examined. In the case of medium containing exogenous  $\text{H}_2\text{O}_2$ , two evolution phases of volume ratio were observed in Fig. 5a. The first one confirms a growth inhibition observed during the first day that is associated with dead cells detachment subsequent to DNA injury induced by  $\text{H}_2\text{O}_2$ . The second phase occurring systematically the second day and during which the spheroids have a greater growth dynamics than the control one (positive slope of daily volume ratio evolution of spheroids treated with  $\text{H}_2\text{O}_2$ ). Figure 5b shows that exogenous  $\text{H}_2\text{O}_2$  induces DNA damage in  $\text{H}_2\text{O}_2$  concentration-dependent manner. Comparison of the extend of DNA damage observed in spheroid grown in PAM (Fig. 1b) or in the presence of added exogenous  $\text{H}_2\text{O}_2$  (Fig. 5b) suggests that  $\text{H}_2\text{O}_2$  concentration in plasma-activated culture medium for  $T_{exp} = 120$  s is between 0.5 and 2.5 mM.

This result demonstrates that the addition of exogenous  $\text{H}_2\text{O}_2$  induces DNA damage the first day but this is not sufficient to obtain both DNA damage and growth inhibition of MCTS. This underlines that treatment of cancer cells with only exogenous  $\text{H}_2\text{O}_2$  cannot stop growth inhibition thus underlying the central role of the other plasma byproducts generated in the liquid media.

**Growth inhibition and genotoxic activity of PAM are retained during 7 days of storage at either  $+4\ ^\circ\text{C}$  or  $-80\ ^\circ\text{C}$ .** Preservation of PAM growth inhibition and genotoxic activities as a function of temperature of storage was examined. To this aim, PAM was prepared after exposure to He plasma jet during 120 s, then stored during 7 days at different temperature conditions  $+37\ ^\circ\text{C}$ ,  $+4\ ^\circ\text{C}$ ,  $-20\ ^\circ\text{C}$  and  $-80\ ^\circ\text{C}$ , and used to grow spheroids for 4 hours. Figure 6b displays DNA damage detection 24 h after MCTS treatment with PAM stored at the indicated temperatures. Quantitative analysis of fluorescence images shows that about 36% of spheroid volume presents DNA damage with PAM stored at  $+4\ ^\circ\text{C}$ . This volume is about 44% when PAM was stored at  $-80\ ^\circ\text{C}$ . The ability of PAM to induce DNA damage was not changed after 7 days of storage at temperature of either  $+4\ ^\circ\text{C}$  or  $-80\ ^\circ\text{C}$ . In contrast, this genotoxic activity disappears in the case of PAM stored of  $+37\ ^\circ\text{C}$  or  $-20\ ^\circ\text{C}$ .

These results suggest that  $\text{H}_2\text{O}_2$  concentration in PAM remains stable during at least 7 days of storage at  $+4\ ^\circ\text{C}$  and  $-80\ ^\circ\text{C}$  while  $\text{H}_2\text{O}_2$  is certainly decomposed when PAM was stored at  $+37\ ^\circ\text{C}$  and  $-20\ ^\circ\text{C}$ . Growth inhibition effect displayed in Fig. 6a confirm DNA damage results. In the cases of PAM stored at  $+4\ ^\circ\text{C}$  and  $-80\ ^\circ\text{C}$ , the volume loss can reach about 50% due to cells detachment presenting DNA damages during the first day. The volume of spheroids treated with PAM stored at  $+37\ ^\circ\text{C}$  and  $-20\ ^\circ\text{C}$  can also reaches 50% but only after several days in contact with PAM (Fig. 6b). This inhibitory effect of PAM on spheroid growth remains similar whatever

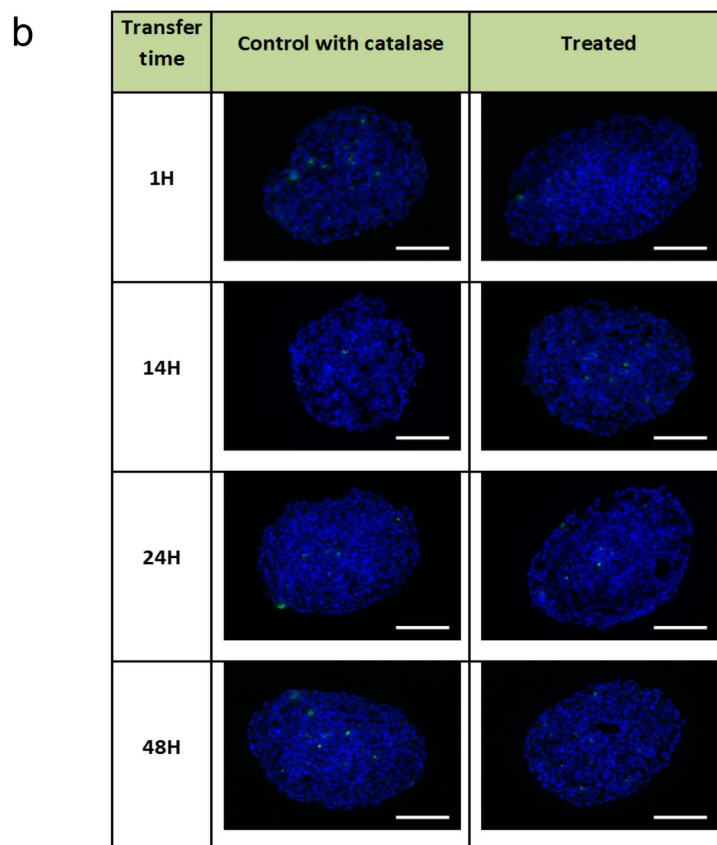
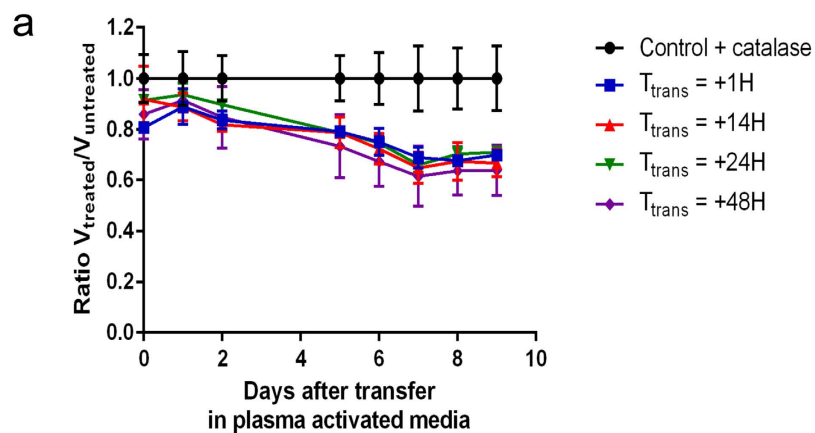


**Figure 3. Growth inhibition and genotoxic effects of PAM in the presence of catalase.** (a) Variation of the relative volume of HCT116 spheroids grown in plasma-activated media in the presence of catalase ( $30\mu\text{g}\cdot\text{mL}^{-1}$ ). Spheroids were cultured during five days in DMEM and subjected to plasma-conditioned medium at day 0 for several transfer time  $T_{\text{trans}}$ . Data are shown as means  $\pm$  SD from four independent experiments. (b) Genotoxic effect of PAM detected 4 h after transfer time of MCTS in PAM. Immuno-detection of the phosphorylation of the histone variant H2AX (phospho-H2AX, green) on  $5\mu\text{m}$  cryosections of control or treated spheroids. DAPI (blue) correspond to the Nuclei. Data shown are representative images from four independent experiments. Scale bar,  $100\mu\text{m}$ .

Scavenger	Trapped species	Concentration of scavenger
SOD	$\text{O}_2^{\bullet-}$	150 U/well
D-mannitol	$\text{OH}^{\bullet}$	2.38 mM
L-histidine	$\text{O}_2$ singlet	2.38 mM

**Table 1. Concentration of free-radical scavengers added in culture medium before plasma treatment.**

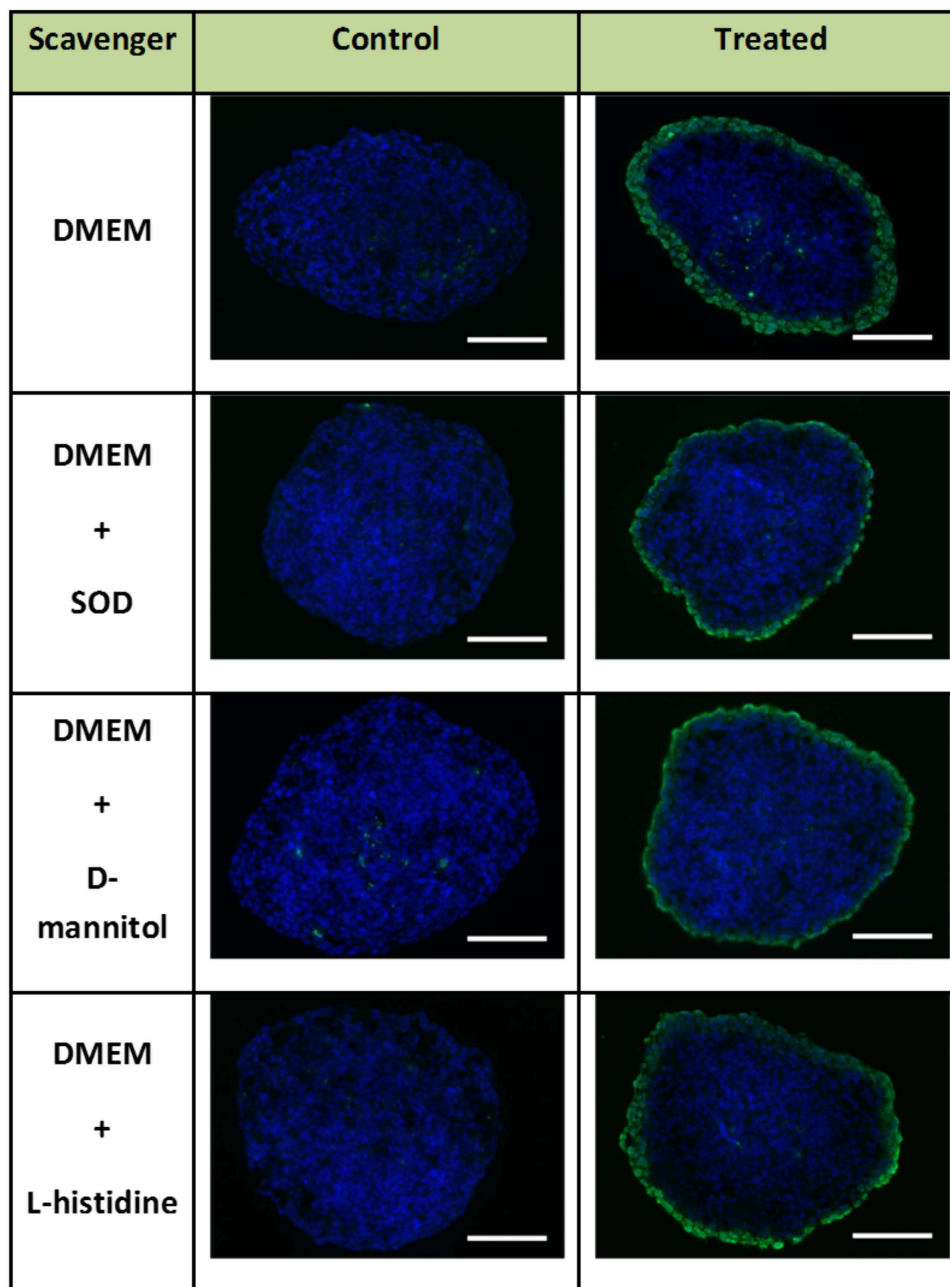


**Figure 4. Genotoxic effect of PAM prepared of with free-radical scavengers.** Immunodetection of DNA damage using antibodies against the phosphorylated form of the histone variant H2AX (phospho-H2AX, green) on 5  $\mu\text{m}$  cryosections from control or treated spheroids fixed 4 h after transfer of MCTS in plasma-activated medium ( $T_{\text{exp}} = 120$  s and  $T_{\text{trans}} = 1$  hour). DAPI (blue) correspond to the Nuclei. Data shown are representative images from four independent experiments. Scale bar, 100  $\mu\text{m}$ .

the storage temperatures suggesting that the concentration of the species responsible of growth inhibition does not depend on the PAM temperature storage.

### Discussion

In the present work, we analyzed the effects of plasma-activated media on the growth inhibition and DNA damage on HCT 116 colon adenocarcinoma multicellular tumor spheroids. PAM is generated by low temperature plasma jet using helium carrier gas operating in open air during several chosen exposure times ( $T_{\text{exp}}$  varying between 60 s to 240 s). The spheroids are grown in PAM after different transfer times ( $T_{\text{trans}}$ ) chosen between 4 hours to 7 days.

We first confirmed and extended our previous findings<sup>20</sup> concerning the growth inhibition of PAM on MCTS. We reported a strong link between DNA damage of MCTS volume and the transfer time of PAM when it is firstly exposed to plasma during 120 s and stored at +37 °C. This genotoxic activity can be observed 24 h after PAM

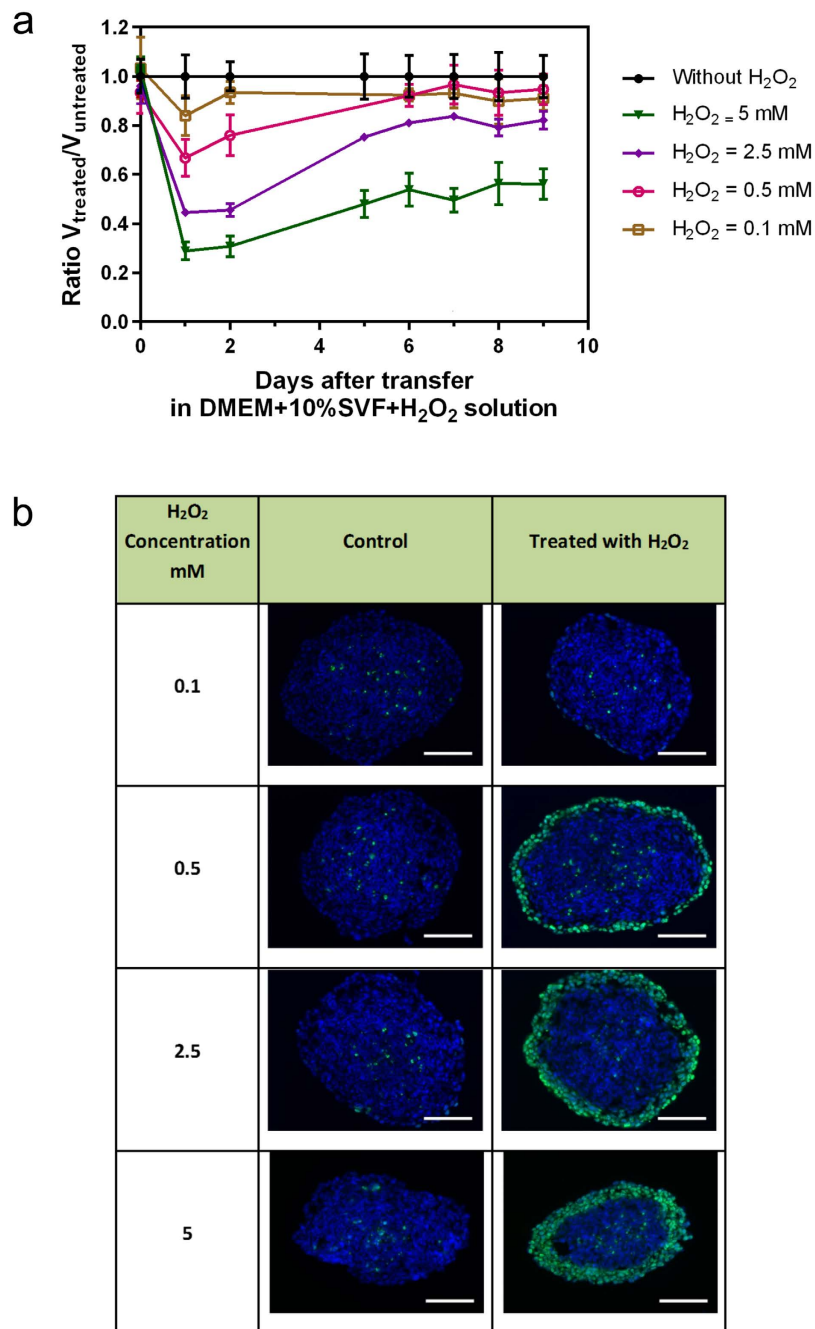


**Figure 5. Growth inhibition and genotoxic effects of hydrogen peroxide exogenously added to culture media in MCTS.** (a) The time-evolution of the growth of HCT116 spheroids after their transfer into culture medium in the presence of increasing concentration of exogenous hydrogen peroxide. Spheroids were cultured five days in DMEM and then transferred in culture medium containing H<sub>2</sub>O<sub>2</sub> at day 0. Data are shown as means  $\pm$  SD from four independent experiments (b) DNA damage due to hydrogen peroxide concentration added in culture media without any plasma treatment. Genotoxicity is analyzed by immunodetection of the phosphorylation of the histone variant H2AX (phospho- H2AX, green) on 5  $\mu$ m cryosections of control HCT116 MCTS or MCTS for transfer time T<sub>trans</sub> 1 h. DAPI (blue) correspond to the Nuclei. Data shown are representative images from four independent experiments. Scale bar, 100  $\mu$ m.

activation. In contrast, growth inhibition effect is also observed for all transfer times. These results indicate that the observed effects of PAM on multicellular spheroids is due to the accumulation of long lifetime chemically reactive species generated in PAM during plasma short exposure time (equal to 120 s). PAM efficiency on spheroids are therefore dependent on transfer time and exposure time. Similar dependence has been also recently shown by Mohades<sup>38</sup> in the case of monolayer cultured (or 2D) model of carcinoma cell.

The quantitative analysis of fluorescence images has shown that the decrease of volume ratio can be correlated to the loss of peripheral spheroid cells displaying DNA damage as already underlined in our previous work<sup>20</sup>. The

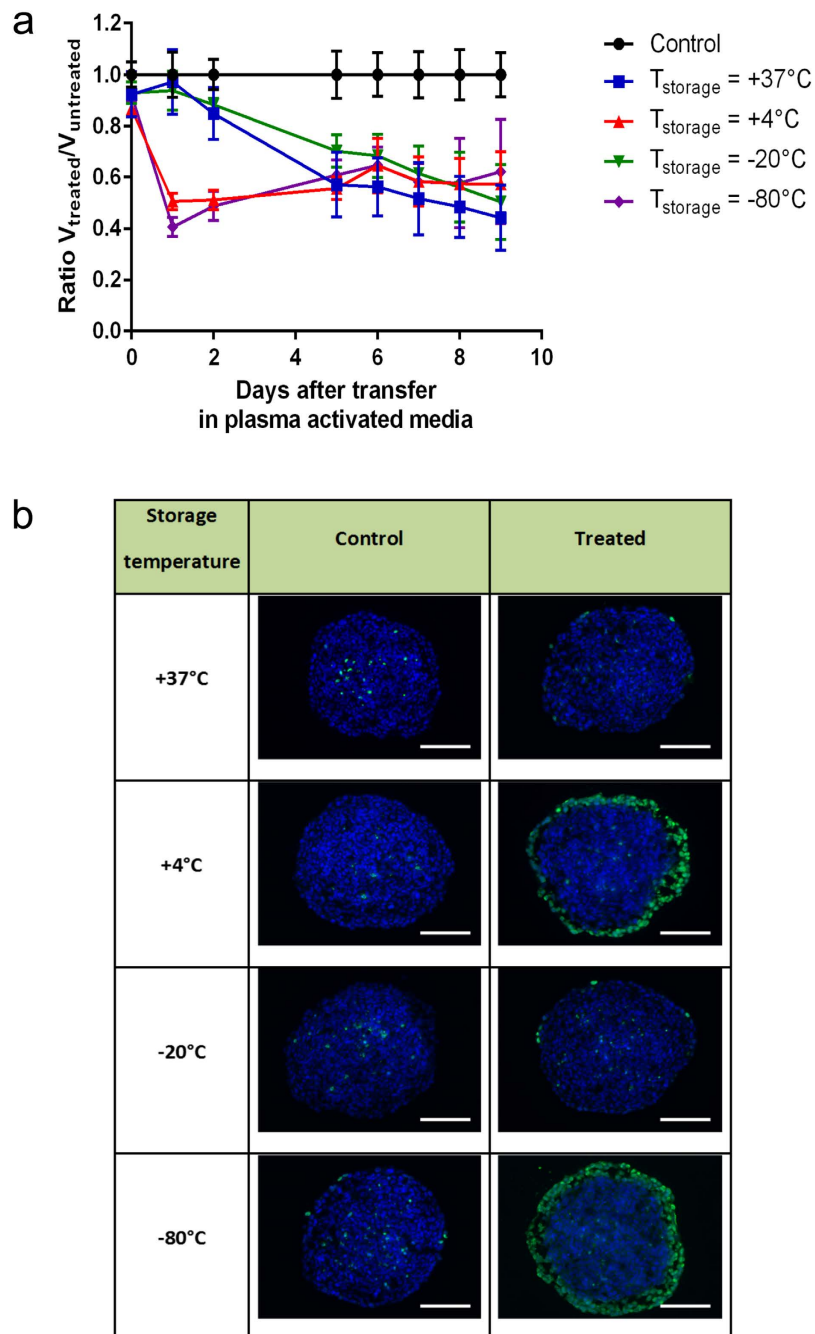


**Figure 6. Growth inhibition and genotoxic effects of PAM stored at different temperatures. (a)** Evolution of volume ratio of MCTS grown in PAM activated during  $T_{exp} = 120$  s and stored at different temperature during 7 days:  $+37^\circ\text{C}$ ,  $+4^\circ\text{C}$ ,  $-20^\circ\text{C}$  and  $-80^\circ\text{C}$ . Spheroids were cultured five days in DMEM and then transferred in PAM at day 0. Data are shown as means  $\pm$  SD from four independent experiments. **(b)** Genotoxic effect of PAM detected by immunodetection of the phosphorylation of the histone variant H2AX (phospho-H2AX, green) on  $5\ \mu\text{m}$  cryosections from control spheroids or treated spheroids 4 h after transfer of MCTS in PAM (exposure time to plasma jet  $T_{exp} = 120$  s and time transfer inside PAM  $T_{trans} = 7$  days). DAPI (blue) correspond to the Nuclei. Data shown are representative images from four independent experiments. Scale bar,  $100\ \mu\text{m}$ .

reduction in the volume ratio means that all the cells subjected to DNA damage will then detach from the spheroids to die either by necrotic or apoptotic pathway. Moreover, when there are minor and/or manageable DNA damage the microscopy observation do not show any cell detachment but growth inhibition is still observed. This confirms that cytotoxic species in PAM can induce cell growth inhibition without DNA damage.

In our previous work<sup>20</sup>, we demonstrated that reactive oxygen species (ROS) are involved in the DNA damaging effect detected in MCTS in the case of treatment by direct exposure to the plasma jet. The experiments reported here with and without catalase scavenger suggest that  $\text{H}_2\text{O}_2$  is the main agent involved in the observed



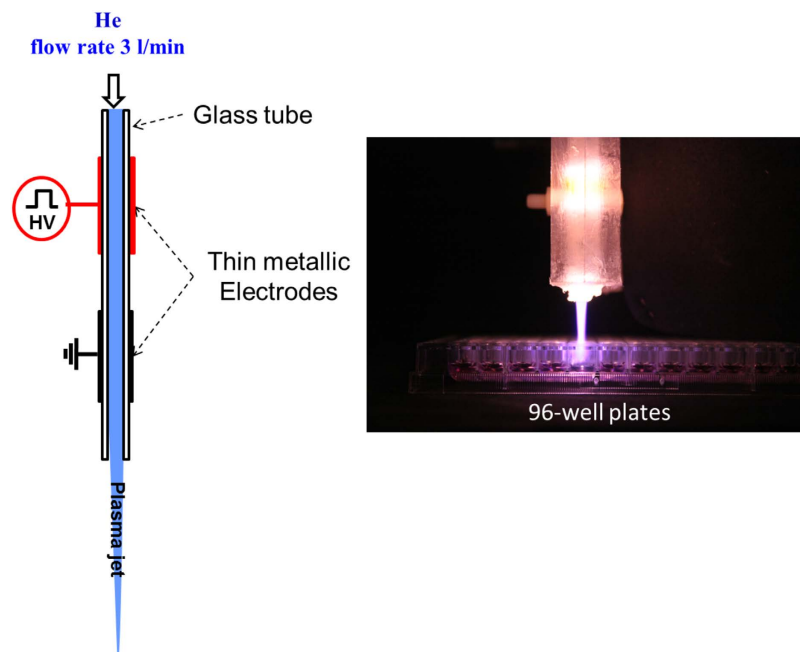


**Figure 7. Experimental setup.** In the left side: Illustrative set-up low temperature plasma jet using dielectric barrier discharge by mono-polar pulsed high-voltage power (voltage = 9 kV, repetition rate = 10 kHz, pulse width = 1  $\mu$ s), and using helium flowing gas at 3 liter  $\text{min}^{-1}$  in the upstream side. In the right side: Preparation of PAM by exposition of 100  $\mu$ L culture medium in 96-well plates to the low-temperature Helium plasma jet. Distance between culture medium and the top of the quartz tube is fixed at 2 cm.

DNA damage. Furthermore, by comparison between the effect of non-activated medium supplemented with exogenous  $\text{H}_2\text{O}_2$ , the concentration of  $\text{H}_2\text{O}_2$  produced in plasma-activated culture medium for  $T_{\text{exp}} = 120$  s was estimated to be between 0.5 and 2.5 mM. Fluorimetric Hydrogen Peroxide Assay Kit (Sigma) was used to validate the estimated concentration of hydrogen peroxide produced by plasma jet in culture medium. For 120 s exposure time, the measured concentration of  $\text{H}_2\text{O}_2$  is  $1.05 \pm 0.09$  mM. This result shows a good coherence between the two methods of hydrogen peroxide quantification.

In addition, in the absence of  $\text{H}_2\text{O}_2$ , moderate growth inhibition effect was still observed. These growth inhibitory effects can be likely associated with other radical species with a long lifetime formed during the generation of PAM when exposed to the plasma jet. Radical species may be involved in this growth inhibitory effect can include reactive nitrogen species (RNS)<sup>39</sup> and/or the chemical change of amino acids present in the medium induced by plasma radical species<sup>40</sup>.

One important factor of the potential clinical application of PAM is its stability during storage. We reported here that PAM maintains its genotoxic activity during storage at either +4  $^{\circ}\text{C}$  or -80  $^{\circ}\text{C}$  during at least 7 days. The conservation of PAM genotoxic activity during this period of 7 days is in agreement with literature results<sup>28</sup> in the case of the temperature storage of -80  $^{\circ}\text{C}$  but not for +4  $^{\circ}\text{C}$  which is the recommended temperature to store the manufactured hydrogen peroxide to avoid its decomposition. This can be due to the ability of  $\text{H}_2\text{O}_2$  molecule to remain stable at +4  $^{\circ}\text{C}$  or at a temperature lower than -60  $^{\circ}\text{C}$  leading to the  $\text{H}_2\text{O}_2$  crystallization state (according to the classical diagram phase<sup>41</sup>) thus avoiding its chemical decomposition and therefore preserving its capability to induce DNA damage to spheroids. This shows one more time the important genotoxic role played by  $\text{H}_2\text{O}_2$  plasma induced in PAM. Furthermore, PAM stored during the same duration of 7 days has maintained also its growth inhibition properties. In conclusion, we demonstrated that PAM has both genotoxic and cytotoxic effects on HCT116 colon adenocarcinoma multicellular tumor spheroids when stored at appropriate temperature (e.g. +4  $^{\circ}\text{C}$ ). Forthcoming work will have to be devoted to further investigate the identity of the genotoxic and cytotoxic aqueous species using electron spin resonance.

## Materials and Methods

**Low temperature plasma jet at atmospheric pressure.** Low temperature plasma jet is generated by using dielectric barrier discharge previously described elsewhere<sup>20,42</sup>. In short, plasma discharges are produced in a quartz tube (4 mm and 6 mm for respectively inner and outer diameters) on which two aluminum tape electrodes having 20 mm width are wrapped and separated by 10 mm gap. Helium gas carrier is injected with a flow rate of 3 sl/min. The electric discharge is ignited by mono-polar square pulses 9 kV of voltage magnitude, 10 kHz of frequency and 1  $\mu$ s duration of square pulse.

Figure 7 displays a illustrative view of the plasma jet device and an example of plasma exposure of 100  $\mu$ L culture medium in a well of 96-round bottom well cell culture plates. The gas temperature estimated around 30  $^{\circ}\text{C}$  using emission spectroscopy based on OH(A-X) molecular spectra. Furthermore, generation of ROS, such

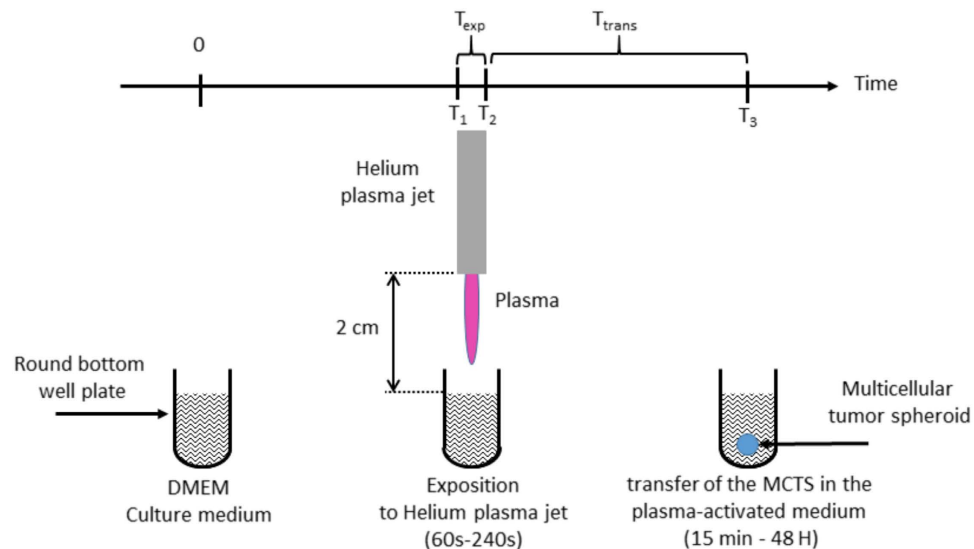


**Figure 8.** Main steps of the experimental procedure displaying (1) at time = 0, the well containing 100  $\mu$ l of the liquid medium before the plasma exposure, (2) the preparation of PAM corresponding to the duration of the exposure of the culture media to low temperature plasma jet ( $T_{exp}$ ) and (3) the delay ( $T_{trans}$ ) between the end of plasma exposure and transfer of MCTS in this conditioned media.

as hydroxyl radicals, singlet oxygen radicals, nitrogen oxide, and nitrogen, were confirmed by optical emission spectroscopy<sup>20</sup>.

**Cell culture and spheroids generation.** HCT116 colorectal cancer cells (ATCC) were cultured in growth medium (DMEM (Invitrogen) supplemented with 10% Fetal Calf Serum (FCS) and 2  $mL^{-1}$  glutamine and penicillin/streptomycin) in 5%  $CO_2$  humidified atmosphere at 37  $^{\circ}C$ <sup>20</sup>. Centrifugation method was used to generate spheroids in low attachment multi-well plates, as previously described<sup>20,43</sup>. In short, 500 cells/well were collected and distributed in poly-HEMA-coated 96-round bottom well plates. Following centrifugation (600 g during 6 min) the plates were placed in a humidified atmosphere of 5%  $CO_2$  at 37  $^{\circ}C$ . By using this technique single spheroids were obtained in each well and the size variation between spheroids is less than 10%. When the diameter of spheroids is about 400  $\mu m$  (measured by using calibrated eyepiece reticule), the plasma treatment can be started.

**Immunofluorescence on spheroid cryosections.** After PAM treatment, neutral-buffered formalin (Sigma) was used to fix spheroids during 2 h, the spheroids were rinsed with PBS (phosphate buffer saline) and stored at 4  $^{\circ}C$ <sup>20</sup>. After fixation, PBS with 15% and then 30% of sucrose was used to incubate spheroids at 4  $^{\circ}C$  during 24 h. The latter were embedded in Tissue-Tek (Sakura Finetek) and then cut in 5  $\mu m$ -thick cryosections. After a blocking step in PSB, 10% SVF, 0.5% Triton X-100, spheroid sections were incubated with antibodies against phosphorylated Histone H2AX (mouse monoclonal, Millipore, 1/500 one hour at 37  $^{\circ}C$ ). After washes in PBS/0.1% Triton X-100 v/v, the secondary antibody was added for 1 h (anti-mouse conjugated with Alexa 488, Molecular Probes, 1/800, at room temperature). DNA was stained using 4', 6-diamidino-2-phénylindole (DAPI)<sup>20</sup>.

**Image processing and analysis.** As previously depicted<sup>20</sup>, epifluorescence microscope DM5000 (Leica) equipped with CCD camera (Roper COOLsnap ES) was used to collect fluorescence images of spheroid sections of 5  $\mu m$  thickness. Software packages (Metavue and ImageJ) were then used to process fluorescence.

**Data statistics.** The reported data correspond to the mean  $\pm$  SD (standard deviation) of at least three independent experiments for the untreated spheroids and four independent experiments for the treated spheroids. Student's test was used to perform statistical analysis.

**Production of plasma activated medium (PAM) and cell treatment.** Conditioned culture medium, designated by PAM, was produced through the exposure of cell culture media to low temperature plasma jet using helium carrier gas. Figure 8 shows a diagram depicting the experimental setup. The complete culture medium made from DMEM with 10% FCS and 2  $mL^{-1}$  glutamine and penicillin/streptomycin. DMEM was exposed to the plasma jet in 96-wells plates (100  $\mu L$  per well) for duration ranging from 60 s to 240 s (Time exposure,  $T_{exp}$ ). For data reproducibility, all plasma exposures were performed under the same experimental conditions (applied voltage, frequency, pulse duration and gas flow), same distance  $d$  ( $d = 2$  cm) between plasma jet tube output and the upper-surface of liquid medium (see Fig. 8). A concealing plate (not illustrated in fig. 7) was always used to mask neighboring wells to avoid cross-exposure during the plasma exposure. 96-wells plates containing PAM were then stored in a humidified atmosphere of 5%  $CO_2$  at 37  $^{\circ}C$ .

HCT116 spheroids were transferred in PAM immediately after its preparation or after a selected delay subsequently referred as Time transfer Ttrans (Ttrans = 1 h, 14 h, 24 h and 48 h) (Fig. 8). The spheroid size is about 400  $\mu\text{m}$  diameter when it is transferred in PAM. At that stage a proliferation gradient starts to organize with quiescent cells in the inner layers. No necrotic core is detected and will appear at later stages of growth.

## References

- Laroussi, M. Non-thermal decontamination of biological media by atmospheric pressure plasmas: review, analysis, and prospects. *IEEE Trans Plasma Sci* **30**, 1409–1415 (2002).
- Lu, X. & Laroussi, M. Dynamics of an atmospheric pressure plasma plume generated by submicrosecond voltage pulses. *J Appl Phys* **100**, 063302 (2006).
- Lu, X. *et al.* An 11 cm long atmospheric pressure cold plasma plume for applications of plasma medicine. *Appl Phys Lett* **92**, 081502 (2008).
- Yousfi, M., Eichwald, O., Merbahi, N. & Jomaa, N. Analysis of ionization wave dynamics in low-temperature plasma jets from fluid modeling supported by experimental investigations. *Plasma Sources Sci Technol* **21**, 045003 (2012).
- Duan, Y., Huang, C. & Yu, Q. Low-temperature direct current glow discharges at atmospheric pressure. Plasma Science. *IEEE Trans Plasma Sci* **33**, 328–329 (2005).
- Dudek, D., Bibinov, N., Engemann, J. & Awakowicz, P. Direct current plasma jet needle source. *J Phys D: Appl Phys* **40**, 7367 (2007).
- Stoffels, E., Flikweert, A. J., Stoffels, W. W. & Kroesen, G. M. W. Plasma needle: a non-destructive atmospheric plasma source for fine surface treatment of (bio) materials. *Plasma Sources Sci Technol* **11**, 383–388 (2002).
- Lee, H. W. *et al.* Synergistic sterilization effect of microwave-excited nonthermal Ar plasma, H<sub>2</sub>O<sub>2</sub>, H<sub>2</sub>O and TiO<sub>2</sub>, and a global modeling of the interactions. *Plasma Sources Sci Technol* **22**, 055008 (2013).
- Choi, J., Iza, F., Do, H. J., Lee, J. K. & Cho, M. H. Microwave-excited atmospheric-pressure microplasmas based on a coaxial transmission line resonator. *Plasma Sources Sci Technol* **18**, 025029 (2009).
- Calzada, M. D., Saez, M. & Garcia, M. C. Characterization and study of the thermodynamic equilibrium departure of an argon plasma flame produced by a surface-wave sustained discharge. *J Appl Phys* **88**, 34 (2000).
- Ogawa, Y. *et al.* An epoch-making application of discharge plasma phenomenon to gene-transfer. *Biotechnol Bioeng* **92**, 865–870 (2005).
- Yousfi, M., Merbahi, N., Pathak, A. & Eichwald, O. Low-temperature plasmas at atmospheric pressure: toward new pharmaceutical treatments in medicine. *Fundam Clin Pharmacol* **28**, 123–135 (2014).
- Fridman, G. *et al.* Applied plasma medicine. *Plasma Process Polym* **5**, 503–533 (2008).
- Heinlin, J. *et al.* Plasma medicine: possible applications in dermatology. *J Dtsch Dermatol Ges* **8**, 968–976 (2010).
- Desmet, T. *et al.* Non thermal plasma technology as a versatile strategy for polymeric biomaterials surface modification: a review. *Biomacromolecules* **10**, 2351–2378 (2009).
- Kong, M. G. *et al.* Plasma medicine: an introductory review. *New J Phys* **11**, 115012 (2009).
- Ishaq, M., Evans, M. M. & Ostrikov, K. K. Effect of atmospheric gas plasmas on cancer cell signaling. *Int J Cancer* **134**, 1517–1528 (2014).
- Koritzner, J. *et al.* Restoration of sensitivity of chemo-resistant glioma cells by cold plasma atmospheric pressure. *PLoS One* **8**, e64498 (2013).
- Vandamme, M. *et al.* ROS implication in a new anti-tumor strategy based on non thermal plasma. *Int J Cancer* **130**, 2185–2194 (2012).
- Plewa, J. *et al.* Low temperature plasma-induced antiproliferative effects on Multicellular Tumor Spheroid. *New J Phys* **16**, 043027 (2014).
- Tuhvatulin, A. I. *et al.* Non thermal plasma causes pr53- dependent apoptosis in human colon carcinoma cells. *Acta Naturae* **4**, 82–87 (2012).
- Ahn, H. J. *et al.* Atmospheric pressure plasma jet induces apoptosis involving mitochondria via generation of free radicals. *PLoS One* **6**, e28154 (2011).
- Wang, M. *et al.* Cold Atmospheric Plasma for Selectively Ablating Metastatic Breast Cancer Cells. *PLoS One* **8**, e73741 (2013).
- Keidar, M. *et al.* Cold plasma selectivity and possibility of a paradigm shift in cancer therapy. *British Journal of Cancer* **105**, 1295–1301 (2011).
- Kim, J. Y., Kim, S. O., Wei, Y. & Li, J. A flexible cold micro-plasma jet using biocompatible dielectric tubes for cancer therapy. *Appl Phys Lett* **96**, 203701 (2010).
- Volotskova, O., Hawley, T. S., Stepp, M. A. & Keidar, M. Targeting the cancer cell cycle by cold atmospheric plasma. *Sci Rep* **2**, 636 (2012).
- Tanaka, H. *et al.* Cell survival and proliferation signaling pathways are downregulated by plasma activated medium in glioblastoma brain tumor cells. *Plasma Med* **2**, 207–220 (2012).
- Adachi, T. *et al.* Plasma-activated medium induces A549 cell injury via a spiral apoptotic cascade involving the mitochondrial–nuclear network. *Free Radic Biol Med* **79**, 28–44 (2015).
- Utsumi, F. *et al.* Selective cytotoxicity of indirect nonequilibrium atmospheric pressure plasma against ovarian clear cell carcinoma. *SpringerPlus* **3**, 398 (2014).
- Utsumi, F. *et al.* Effect of indirect nonequilibrium atmospheric pressure plasma on anti proliferative activity against chronic chemo resistant ovarian cancer cells *in vitro* and *in vivo*. *PLoS One* **8**, e81576 (2013).
- Ye, F. *et al.* Plasma-activated medium suppresses choroidal neovascularization in mice: a new therapeutic concept for age-related macular degeneration. *Sci Rep* **5**, 7705 (2015).
- Pampaloni, F., Reynaud, E. G. & Stelzer, E. H. The third dimension bridges the gap between cell culture and live tissue. *Nat Rev Mol Cell Biol* **8**, 839–845 (2007).
- Xu, D. *et al.* *In Situ* OH Generation from O<sub>2</sub><sup>-</sup> and H<sub>2</sub>O<sub>2</sub> Plays a Critical Role in Plasma-Induced Cell Death. *PLoS One* **10**, e0128205 (2015).
- Chelikani, P., Fita, I. & Loewen, P. C. Diversity of structures and properties among catalases. *Cell Mol Life Sci* **61**, 192–208 (2004).
- Baehner, R. L., Murrmann, S. K., Davis, J. & Johnston Jr, R. B. The role of superoxide anion and hydrogen peroxide in phagocytosis-associated oxidative metabolic reactions. *J Clin Invest* **56**, 571–576 (1975).
- Wu, H. *et al.* Reactive Oxygen Species in a Non-thermal Plasma Microjet and Water System: Generation, Conversion, and Contributions to Bacteria Inactivation—An Analysis by Electron Spin Resonance Spectroscopy. *Plasma Process Polym* **9**, 417–424 (2012).
- Ikeda, Y. *et al.* L-Histidine but not D-Histidine Attenuates Brain Edema Following Cryogenic Injury in Rats. *Acta Neurochir Suppl* **76**, 195–197 (2000).
- Mohades, S., Laroussi, M., Sears, J., Barekzi, N. & Razavi, H. Evaluation of the Effects of a Plasma Activated Medium on Cancer Cells. *Phys. Plasmas* **22**, 122001 (2015).
- Machala, Z., Tarabova, B., Hensel, K., Spetlikova, E., Sikurova, L. & Lukes, P. Formation of ROS and RNS in water Electro-Sprayed through Transient Spark Discharge in Air and their Bactericidal Effects. *Plasma Process Polym* **10**, 649–659 (2013).

40. Takai, E *et al.* Chemical modification of amino acids by atmospheric-pressure cold plasma in aqueous solution. *J Phys D: Appl Phys* **47**, 285403 (2014).
41. Giguère, P. A. & Secco, E. A. Hydrogen peroxide and its analogues: V. phase equilibria in the system D<sub>2</sub>O-D<sub>2</sub>O<sub>2</sub>. *Can. J. Chem.* **32**, 550–556 (1954).
42. Yousfi, M., Eichwald, O., Merbahi, N. & Jomaa, N. Analysis of ionization wave dynamics in low-temperature plasma jets from fluid modeling supported by experimental investigations. *Plasma Sources Sci Technol* **21**, 045003 (2012).
43. Laurent, J. *et al.* Multicellular tumor spheroid models to explore cell cycle checkpoints in 3D. *BMC Cancer* **13**, 73 (2013).

## Acknowledgements

Université Paul Sabatier, CNRS, Région Midi-Pyrénées and Agence Nationale de la Recherche ANR (12-BSV5-0008-01) have supported this work. We also acknowledge the TRI-Genotoul and ITAV imaging facilities.

## Author Contributions

E.J. performed research, prepared all figures and provided assistance in manuscript writing. C.F. provided assistance with spheroids culture and cytotoxic and genotoxic techniques. B.D. provided assistance of cytotoxic and genotoxic analysis results and in manuscript writing. M.Y. provided data analysis and interpretation and assistance in manuscript writing. V.L. provided assistance with spheroids culture, cytotoxic and genotoxic analysis and in manuscript writing. N.M. conceived and supervised the study project, provided data analysis and interpretation and wrote the manuscript.

## Additional Information

**Competing financial interests:** The authors declare no competing financial interests.

**How to cite this article:** Judée, F. *et al.* Short and long time effects of low temperature Plasma Activated Media on 3D multicellular tumor spheroids. *Sci. Rep.* **6**, 21421; doi: 10.1038/srep21421 (2016).



This work is licensed under a Creative Commons Attribution 4.0 International License. The images or other third party material in this article are included in the article's Creative Commons license, unless indicated otherwise in the credit line; if the material is not included under the Creative Commons license, users will need to obtain permission from the license holder to reproduce the material. To view a copy of this license, visit <http://creativecommons.org/licenses/by/4.0/>